

# ***In vitro* evaluation of drug release and antibacterial activity of a silver-loaded wound dressing coated with a multilayer system**

Alejandra Mogrovejo-Valdivia<sup>a</sup>, Oumaira Rahmouni<sup>a,b</sup>, Nicolas Tabary<sup>c</sup>, Mickael Maton<sup>a</sup>, Christel Neut<sup>b</sup>, Bernard Martel<sup>c</sup>, Nicolas Blanchemain<sup>a\*</sup>

<sup>a</sup> Univ. Lille, INSERM, CHU Lille, U1008 - Controlled Drug Delivery Systems and Biomaterials, F-59000 Lille, France

<sup>b</sup> Univ. Lille, INSERM, CHU Lille, U995- LIRIC - Lille Inflammation Research International Center, F-59000 Lille, France

<sup>c</sup> Univ. Lille, CNRS UMR8207, UMET - Unité Matériaux et Transformations, F-59655 Villeneuve D'Ascq, France

\* Corresponding author. Dr. Nicolas Blanchemain

E-mail : [nicolas.blanchemain@univ-lille2.fr](mailto:nicolas.blanchemain@univ-lille2.fr)

Address: INSERM U1008, Controlled Drug Delivery Systems and Biomaterials, College of Pharmacy, University of Lille, 59006 Lille, France

Tel.: +33 320 62 69 75

Fax: +33 320 62 68 54

## **Abstract**

The goal of the study was to elaborate an antibacterial silver wound dressing covered by a protective coating that would prevent silver diffusion toward skin without losing its biocide properties. Therefore, non woven polyethyleneterephthalate (PET) textiles were pre-treated by two types of polysaccharides – chitosan and cyclodextrin – both crosslinked with citric acid by a pad/dry/cure process. Both types of resulting thermofixed textiles carrying the citrate crosslinks were then impregnated in silver solution followed by a thermal treatment and were finally coated by Layer-by-Layer (L-b-L) deposition of a polyelectrolyte multilayer (PEM) film consisting of anionic water-soluble poly-cyclodextrin and cationic chitosan. The influence of the process parameters was investigated in terms of silver adsorption capacity, PEM system build-up, silver kinetics of release and antibacterial activity. We demonstrate i) the utility of the intermediate thermal treatment step in the reduction of silver leakage in the polyelectrolyte solutions used in the L-b-L process, ii) that silver adsorption on the preliminary thermofixed layers did not affect the PEM system build-up, iii) the slowing down of silver release kinetic thanks to the PEM coating, iv) the preservation of the antibacterial activity despite the PEM coating.

## 1. Introduction

Infection hinders and delays the wound healing process and can lead to the chronicity of the wound. This problem complicates wound management in terms of cost-effective treatment and patient's quality of life (Jhass et al., 2017). Therefore, preventive measures limiting wound infection are a challenge for public health. The worldwide high use of antibiotics to treat infection (Bhowmick and Koul, 2016) results in a high level of bacterial resistance (Ito et al., 2015; Rai et al., 2012), their use has to be limited. Alternative solutions such as antiseptic dressings are proposed as innovative antibacterial systems. As a matter of fact, the use of silver-based dressings is now widespread as they are indicated for treating declared wound infections or for preventing wound colonization (Atiyeh et al., 2007; Leaper and MacGregor, 2012). Silver has been used for centuries as an antimicrobial agent (Abboud et al., 2014; Marx and Barillo, 2014) due to its broad-spectrum activity against Gram-positive, Gram-negative, aerobic, anaerobic bacteria, fungi, viruses and protozoa (Abdel-Mohsen et al., 2017; Atiyeh et al., 2007; Halstead et al., 2015). Silver in its ionic form ( $\text{Ag}^+$ ) interacts with bacteria by the destruction of the bacterial membrane, the inhibition of DNA replication by interaction with the cytochrome of the respiratory chain causing the death of bacteria (Atiyeh et al., 2007; Leaper and MacGregor, 2012; Marx and Barillo, 2014).

Nowadays, a wide range of wound dressings containing silver are available. Silver is found in dressings in different forms and concentrations. For example, Aquacel® Ag (Convatec) presents silver ions at 1.2% (w/w); Acticoat™ (Smith & Nephew) contains silver nanocrystals at 1.64 mg/cm<sup>2</sup> (Rigo et al., 2012; Verbelen et al., 2014). Mepilex® Ag (Molnlycke Health Care), UrgoTul® Silver, UrgoClean® Silver and UrgoCell® Silver (Urgo Medical), contains silver salts (silver sulfate) at concentrations of 1.2 mg/cm<sup>2</sup> for Mepilex® Ag and of 0.35 mg/cm<sup>2</sup> for the range of Urgo®. Despite the great variety of silver dressings, an apparent lack of their efficacy was stated due to the large amount of silver diffusion into the wound during the first hours of treatment (Rigo et al., 2012). Nevertheless, above a certain concentration threshold, silver presents toxic effects on keratinocytes and fibroblasts (Burd et al., 2007; Poon and Burd, 2004) inhibiting their proliferation (Abboud et al., 2014). Therefore, the silver ions delivered by a dressing needs to be maintained above the Minimal

Inhibitory Concentration (MIC) for bacteria (to eliminate them or prevent bacteria their development,) and below the toxic concentration to preserve the tissues. As a consequence, the development of dressings presenting a controlled release of silver is necessary. The immobilization of silver under the form of nanoparticles (NPs) or salts in a wound dressing can be achieved by its incorporation in the melt polymer before spinning, or by the impregnation of the textile in a silver solution or colloidal suspension. However, in the later case specific strategies have to be developed in order to promote the silver species adsorption onto the fibers with which they display low affinity. Therefore, polysaccharides derivatives carrying chelating or ion exchange properties toward metal ions are widely used as polymer coatings of textile fibers.

Recently, many research studies focused on the development of polyelectrolyte multilayer (PEM) based wound dressings as swelling systems (Abdel-Rahman et al., 2016; Fahmy et al., 2018; Trinca et al., 2017) or as drug delivery systems (Agarwal et al., 2012; Anandhakumar and Raichur, 2013; Lee et al., 2012; Maver et al., 2017; Shukla et al., 2012, 2011). Such PEM were built up by applying the layer-by-layer (L-b-L) technique introduced by Decher et al., (Decher, 1997), based on the dip coating of surfaces alternately in two oppositely charged polyelectrolytes solutions resulting in the superposition of self-assembled polyelectrolyte layers. This strategy was then adapted to textiles supports applied as wound dressings. Fahmy and Abou-Okeil (Fahmy et al., 2018), and Abdel Rahman et al., (Abdel-Rahman et al., 2016) used chitosan and hyaluronic acid to obtain antibacterial fabrics with improved swelling properties to promote wound healing with high level of exudate absorption. Polyelectrolytes complexes systems such as poly(allylamine hydrochloride)/poly(acrylic acid) (Agarwal et al., 2012), Poly( $\beta$ -amino ester)/alginate or chondroitin sulfate (Shukla et al., 2012) and poly(allylamine hydrochloride)/dextran sulfate (Anandhakumar and Raichur, 2013) were used to obtain controlled release properties toward chlorhexidine, diclofenac/vancomycin or silver nanoparticles, in the treatment of infected chronic wounds.

Chitosan (CHT) is a natural polysaccharide obtained from the deacetylation of chitin, this biopolymer is composed of D-2-deoxy-2-acetyl-glucosamine and D-2-deoxy-glucosamine units linked by  $\beta$  (1, 4) binding (Croisier and Jérôme, 2013), the use of CHT is very extensive in materials sciences, biotechnology, pharmaceuticals, tissue engineering and medical devices. In particular, CHT is

biocompatible and presents antibacterial and hemocompatible properties and is a source of glucosamine, a compound involved in the healing process. Therefore, CHT is a good candidate for wound dressing applications. In acidic media, protonation of amino groups occurs and gives to CHT the character of a positive polyelectrolyte fully adapted for the development of a PEM system (Gomes et al., 2015; Han et al., 2014; Lee et al., 2012). Two commercial chitosan - based wound dressings are available: KytoCel<sup>®</sup> from Aspen Medical, Chitoderm<sup>®</sup> from Trusetal GmbH. Chitoderm<sup>®</sup> stimulates the proliferation of fibroblasts for the synthesis of connective tissue (Voncina et al., 2016).

Cyclodextrins (CDs) are a family of torus shaped cyclic oligosaccharides composed of glucopyranose units linked by  $\alpha$  (1, 4) bonds formed during enzymatic degradation of starch. The most commonly used CDs are  $\alpha$ -,  $\beta$ - and  $\gamma$ -CD made of 6, 7 or 8 glucose units respectively (Brewster and Loftsson, 2007; Zhang and Ma, 2013). CDs structure presents a hydrophobic cavity, which allows forming inclusion complexes with the lipophilic part a lot of active molecules while the outer hydroxyl groups promote the solubility of the supramolecular species (Brewster and Loftsson, 2007). The inclusion complex stability is driven by the value of the association constant which determines the ratio between the free and complexed forms of the guest molecule in the medium. CDs present a low toxicity and low immunogenicity (Zhang and Ma, 2013) therefore, they present high interest in pharmaceutical domain where they are used as drug carriers, and in biomaterials applications where they are used to provide not only enhanced reservoir properties to implants, but also to endow sustained release of drugs. (Vermet et al., 2017; Jansook et al., 2018). Beside native  $\alpha$ -,  $\beta$ - and  $\gamma$ -CDs, chemically modified cyclodextrins and especially CDs polymers present enhanced solubilizing power (Tabary et al., 2016) due to the cooperative effect between the CD cavities and the polymeric network in the interactions with the drug i) through inclusion complexation on the one hand , ii) through nonspecific interactions with the polymeric structure, through hydrogen bondings, and iii) through ionic interactions with ionized groups carried by the polymeric backbone on the other hand (Danel et al., 2013; García-Fernández et al., 2013).

The aim of the present work was to develop an innovative silver wound dressing loaded with silver and then coated by a PEM system to treat infected wounds and promote wound healing. The challenge tackled here was to benefit from the PEM coating as a protective layer that would reduce

silver diffusion in the wound without losing the antibacterial activity provided by silver. Upstream, was also necessary to check that silver loading on the anionic substrates would not prevent the subsequent PEM build-up. A polyethylene terephthalate nonwoven textile (PET) was chosen as the dressing support because it is biocompatible and often used as layer-contact dressing (Maver et al., 2015). Two kinds of anionic PET supports carrying carboxylate groups were prepared from the crosslinking using citric acid of two polysaccharides, the first one based on cyclodextrin, and the second based on chitosan (Aubert-Viard et al., 2015; Martin et al., 2013b).

Pre-functionalized anionic PET textiles were then loaded with silver sulfate and then covered by self-assembled PEM systems from the alternate layer-by-layer (L-b-L) deposition of the water-soluble forms of CHT and the citric acid-cyclodextrin polymer (PCD) by using the dip-coating technique.

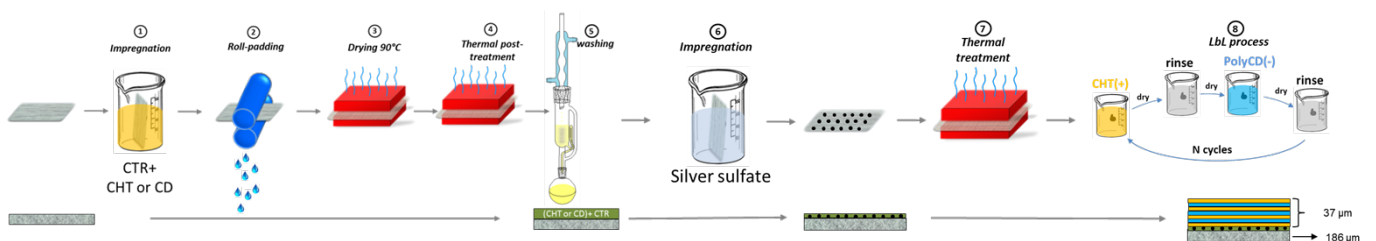


Figure 1 : Representation of the different steps to prepare the silver loaded functionalized textile with a L-b-L system.

The L-b-L coating deposition was followed by the PET textile weight gain versus the number of deposited layers and the characterization was assessed by scanning electronic microscopy (SEM) and energy-dispersive X-ray spectroscopy (EDX). Silver quantification and silver release profiles were assessed by atomic absorption spectroscopy (AAS). Finally, *in vitro* microbiological evaluation was undertaken in order to determine the antibacterial activity of the final wound dressing.

## 2. Materials and Methods

The textile support was a non-woven polyethylene terephthalate textile (PET, reference NSN 365, weight: 65g/m<sup>2</sup>, thickness: 0.186 mm) provided by PGI Nordlys (Bailleul, France). Citric acid monohydrate (CTR, ≥99.5%), sodium hypophosphite monohydrate (NaH<sub>2</sub>PO<sub>2</sub> · H<sub>2</sub>O, ≥ 99%), silver sulfate (Ag<sub>2</sub>SO<sub>4</sub> ≥99%) were purchased by Sigma Aldrich (Saint-Quentin Fallavier, France). Chitosan (CHT, low molecular weight (106 Kg.mol<sup>-1</sup>), viscosity: 146 cP (CHt 1%<sub>w/v</sub> solubilized in 1% acetic acid) with a degree of deacetylation of 77% was supplied by Sigma Aldrich (Saint-Quentin Fallavier, France). Acetic acid (99%) was provided by Merck Millipore.

β-cyclodextrin used in this work was provided by Roquette (Kleptose<sup>®</sup>, Lestrem, France) and the anionic water-soluble polymer of β-cyclodextrin (PCD) was synthesized by solubilization of citric acid, sodium hypophosphite and CDs in respective weight ratios of 10 g/3 g/10 g in 100 mL of water (Martel et al, 2005). After water removal, the solid mixture was then cured at 140°C during 30 min under vacuum. Water was then added, the resulting suspension was filtered, and the filtrate dialyzed during 72 h against water using 6 to 8 kDa membranes (Spectrapor 1, Spectrumlabs). Finally, the water-soluble anionic CD polymer was recovered by freeze drying. The polymer contained 50% in weight of β-cyclodextrin, 4 mmol per gram of COOH groups and the molecular mass was 20 000 g/mol (measured by Size Exclusion Chromatography combined with multi angle light scattering SEC-MALS)

### 2.1. Pre-treatment of PET by pad-dry-cure with citric acid and CHT or CD

Raw PET textile supports were previously washed three times by Soxhlet extractor with isopropanol (3 hours) and rinsed three times with ultrapure water, then dried during 15 minutes at 90°C. Surface modification of PET supports was applied preliminarily to silver loading and L-b-L deposition. Therefore, two different ways for providing anionic character to the nonwoven fibers were applied. In both cases, fibers were modified with carboxylate groups issued from the reaction between citric acid (CTR) and both polysaccharides: chitosan on the one hand, and beta cyclodextrin on the other, hand using the pad/dry/cure process (Aubert-Viard et al., 2015; Martin et al., 2013a, 2013b). Aqueous solution of citric acid (CTR, 10%w/v) and sodium hypophosphite as catalyst (NaH<sub>2</sub>PO<sub>2</sub>, 1%w/v) was prepared. CHT (2.5%w/v) or β-cyclodextrin (10%w/v) was dissolved in the citric acid solution. Weighed raw PET samples (25 cm x 25 cm) were then padded in CHT or β-CD solution,

roll-squeezed (roll speed 1 m/min, 2 bars) (ROACHES, Birstall, England), dried at 90°C for 15 minutes and cured at 140°C in a ventilated oven (Minithermo, Roaches, Birstall, England) for 15 minutes in the case of CHT and for 30 minutes in the case of the  $\beta$ CD. This curing step provoked the crosslinking reaction between each polysaccharide with citric acid (CHT-CTR or CD-CTR). CHT-CTR functionalized textiles were washed with 1%v/v acetic acid solution, and then twice with ultrapure water for 20 minutes. CD-CTR functionalized textiles were washed with ultrapure water three times for 20 minutes under ultrasound. Finally, after washing, all textiles samples were dried at 90°C for 15 minutes. These thermo-fixed primer layers on PET were conventionally named as layer #1 on both supports types named respectively PET-CHT or PET-CD. Finally, in order to transform carboxylic groups (COOH) into carboxylate groups (COO<sup>-</sup>), all samples were treated with a sodium carbonate solution (4 g/L) for 15 minutes then rinsed twice with ultrapure water and finally dried for 15 min at 90°C.

## **2.2. Silver sulfate loading**

PET-CHT or PET-CD textiles were cut in samples of 5x5 cm<sup>2</sup>. Silver sulfate (10 g/L) was dissolved at 70°C under stirring (80 rpm) for 45 minutes and filtered with a polyethersulfone filter (0.22  $\mu$ m, Millex®GP). The textile samples were then impregnated in 65 mL of this solution overnight at 37°C under stirring (80 rpm). Samples were rinsed with ultrapure water in an ultrasonic bath for 1 min and then left under stirring (80 rpm) for 4 min at 37 °C for three times. Samples named PET-CHT-Ag and PET-CD-Ag were dried at 90°C for 15 minutes. Finally, a thermal treatment (TT) was applied at 140°C for 75 minutes; the obtained samples were named PET-CHT-AgTT and PET-CD-AgTT.

## **2.3. Polyelectrolyte multilayer coating**

The PEM system was built according to the method reported by Decher (Decher, 1997; Decher et al., 1998) using the dip-coating technique previously described by our group (Martin et al., 2013a, 2013b). All corresponding samples: PET-CHT, PET-CD, PET-CHT-Ag, PET-CD-Ag, PET-CHT-AgTT and PET-CD-AgTT were firstly dipped into 40 mL of a CHT solution (0.5%w/v) solubilized in acetic acid (1%v/v) for 1, 5 or 15 minutes, dried at 90°C for 15 minutes, rinsed in acetic acid (0.3%v/v) to remove excess of chitosan and finally dried at 90°C for 15 minutes. Then, the samples were dipped into poly-cyclodextrin (PCD) aqueous solution (0.3%<sub>w/v</sub>) for 1, 5, or 15 minutes, dried at 90°C



for 15 minutes, rinsed with ultrapure water for 15 or 5 or 1 minute and dried at 90°C for 15 minutes. The next layers were deposited by applying these sequence “n” times.

The weight gain after each bilayer deposition was calculated using the following equation:

$$WG(\%) = \frac{(m_n - m_i)}{m_i} \times 100$$

where  $m_i$  is the weight of the PET textile after *pad-dry-cure* process and  $m_n$  is the textile weight after each bilayer adsorbed by *dip-coating* method. A treatment at 140°C for 105 minutes was finally applied for the stabilization of the PEM system. These samples were named PET-CHT-AgTT-PEM and PET-CD-AgTT-PEM.

#### **2.4. SEM and EDX analyses**

Textiles samples were analyzed by scanning electronic microcopy (Hitachi S-4700 SEM Field Emission Gun) with an acceleration voltage of 5 kV. The samples were previously treated with a carbon layer to prevent charging. EDX spectra were collected in visually interesting sites to obtain qualitative information on the elemental composition of the surface.

#### **2.5. Silver loading and silver release profile**

The silver content and its release from textile samples were evaluated by flame atomic absorption spectroscopy (AAS) (Thermofisher®) equipped with a silver lamp (328.1 nm) (Thermofisher®). For this purpose, textiles cut into 6 mm diameter disks.

For silver content, textiles were dipped into 10 mL of nitric acid 6.5M overnight at room temperature. Silver concentration was determined from a calibration curve (in the concentration range 2.5 ppm to 25 ppm) and prepared from dilution of a standard silver solution (1000 ppm) (Thermofisher®).

For silver release tests, textile samples were immersed in 2 mL of PBS pH 7.4 at 37°C. Aliquots were withdrawn at different time intervals and then the withdrawn medium was replaced by an equal volume of fresh PBS solution. 2 mL of ammonia at 28% were added to aliquots recovered in order to avoid silver cations salts precipitation. The results were established from the mean of 6 replicates.

#### **2.6. Microbiological evaluation**

##### **2.6.1. Evaluation of the silver action on bacteria**

The microbiological evaluation was determined against *Staphylococcus aureus* (strain CIP224) and *Escherichia coli* (strain K12). Bacterial culture was performed by inoculating a Mueller-Hinton Agar

(MHA) slant incubated for one day at 37°C. A volume of 10 mL of Ringer's cysteinated medium was added to the bacteria culture, then bacteria were removed from the slant. The bacterial suspension contains about  $1 \times 10^9$  CFU (colony forming unit) approximately.

#### **2.6.1.1. Minimal inhibitory concentration (MIC)**

The minimal inhibitory concentration (MIC) of silver sulfate was determined. Briefly, 100  $\mu$ L of Muller-Hinton broth was added in each well of a 96-well microplate (CytoOne®). Then, 100  $\mu$ L of silver sulfate at 400 mg/L was added only on the first well and then serial 2-fold dilutions were carried out directly up to a finally silver sulfate concentration of 0.06  $\mu$ g/L. Then, a volume of 100  $\mu$ L of bacterial suspension at  $1 \times 10^4$  CFU was added to each wells. Plates were incubated at 37°C for 48 h and the MIC was visually determined after 24h and 48h.

#### **2.6.1.2. Bacterial growth curves**

The *S. aureus* and *E. coli* growth behavior exposed to different concentrations of sterile silver sulfate solution was performed. Different tubes containing Muller-Hinton broth, increasing silver sulfate concentration (13, 26, 50, 100 mg/L for *S. aureus* and 5, 10, 15, 20 mg/L for *E. coli*), sterile water and 1 mL of bacterial inocula were incubated at 37°C for 2, 4, 6, 8, 24 and 48 hours. At each interval time a volume of 100  $\mu$ L of each tube is removed and placed on Muller-Hinton agar that were then incubated at 37°C for 24 hours. The number of viable bacteria was counted and expressed as Log CFU mL<sup>-1</sup>.

### **2.6.2. Evaluation of action of the final dressing on bacteria**

#### **2.6.2.1. Kirby-Bauer test**

Kirby-Bauer tests were performed to evaluate the final PEM system in relation for silver release inhibiting bacterial growth. Textile samples (cut into 11 mm diameter disks) and then were dipped in 1 mL of phosphate buffered saline, PBS, pH 7.4 and were then stirring (80 rpm) at 37°C for 72 hours with a daily change of PBS solution. 18 mL of Mueller-Hinton agar (MHA) were poured in Petri dishes ( $\varnothing$ 9 cm). Then, 0.1 mL of the *S. aureus* or *E. coli* at  $1 \times 10^4$  CFU was seeded on the agar. Then, at each interval time, the textiles samples were deposited onto Mueller Hinton agar plates. After 24 hours of incubation at 37°C, the diameter of the inhibition zone is measured and plotted as a function of contact time in PBS.

### **2.6.2.2. Kill-time test**

*Kill-time* test was performed to evaluate the kinetics of the bacterial reduction to determine the antibacterial activity of textiles sample against *S. aureus* and *E. coli* (Aubert-Viard et al., 2015). Textiles samples (11 mm diameter disks) were placed into 24 well plates (CytoOne®). Then, 200  $\mu\text{L}$  of a bacterial suspension ( $1 \times 10^7$  CFU/mL) were placed on the textile samples and the plate was incubated at 37°C. At each interval time (0.5, 2, 4, 6 and 24 hours) the samples were removed from the well and placed in 2 mL of phosphate buffer saline (PBS, pH 7.4), treated in an ultrasonic bath for 1 min and vortexed for 30 seconds to collect the living bacteria. Successive 1/10 dilutions in cysteinated Ringer solution (CR) were made up to  $10^{-4}$  from the recovered bacterial suspension and 0.1 mL of each dilution was seeded onto Mueller-Hinton agar (MHA). The plates were then incubated for 24 h at 37°C. The number of viable bacteria was counted and expressed in Log CFU mL<sup>-1</sup>.

### 3. Results and Discussion

#### 3.1. L-b-L build up on silver loaded wound dressing

First, the textiles samples were functionalized with chitosan or with cyclodextrin both crosslinked with citric acid by using a pad/dry/cure process in order to provide primers layer rich in carboxylate groups (Layer #1). The weight gains measured after this step were  $10.0 \pm 0.7\%$  wt for CHT-CTR modified samples and  $33.0 \pm 5.0\%$  wt for CD-CTR modified samples, corresponding in both cases to COOH groups densities of  $42.1 \pm 9.9 \mu\text{mol} / \text{cm}^2$  and  $13.9 \pm 2.4 \mu\text{mol} / \text{cm}^2$  respectively (Figure 2), determined by the toluidine blue method (Jean-Baptiste et al., Aubert et al.). We have abundantly reported in former papers the crosslinking reaction between cyclodextrin and citric acid, a tricarboxylic compound, that yielded the formation of a crosslinked CD-CTR polymer network that coated the textile fibers. The reaction occurred by esterification of two of the carboxylic functions of CTR with the hydroxyl groups of CD, while the third one remained free and offered cation exchange properties to the support besides the inclusion complexation of properties of the cyclodextrins cavities toward pollutants or drugs (Martel et al., 2002; Ducoroy et al., 2007; Crini et al., Martin et al., 2013; Euvrard et al., 2016).

In the same way, esterification and amidation occurred in case of CHT crosslinking with CTR. In particular, Aubert et al reported that depending on the use of a default or excess of CTR versus CHT, a cationic or anionic textile could be obtained, respectively (Aubert-Viard et al., 2015). In the present case, CTR was used in excess compared to CHT.

Then both types of textiles were loaded with silver considered here as layer #2. The resulting weight gains (figure 2) for this second layer deposition were  $4.26 \pm 1.92\%$  and  $2.5 \pm 0.26\%$  on CD and CHT functionalized textiles respectively. On both primer layers (CHT or CD), silver interacts with residual carboxylic functions carried by the citrate crosslinks (Ducoroy et al., 2008; Aubert-Viard et al., 2015). Besides, in the case of CHT, silver cations are also bound by complexation with the hydroxyl and N-acetyl groups of CHT (Aubert-Viard et al., 2015; Wijesena et al., 2017). After impregnation in the silver solution, a brown coloration appeared on the textiles indicating the binding of the silver ions and their reduction in metallic silver nanoparticles form. The brownish shade increased after the heat treatment at  $140^\circ\text{C}$  during 75 minutes. This phenomenon of conversion of silver salt into silver NPs can be attributed to the reduction of silver ions into silver nanoparticles through mechanisms reported

in literature concerning CHT (Carapeto 2017), and through the common action of heat and cyclodextrin citrate repeat units of the crosslinked network concerning CD (Ma et al. 2016). UV-visible Spectra of Figure 3a and Figure 3b clearly show the interactions between silver and the cyclodextrin polymer or the chitosan in solution by the appearance of the broadband characteristic of the silver nanoparticles between 400 and 600 nm in particular after 24 to 168 hours (Abdel-Mohsen et al., 2017). Ma et al. (Ma et al., 2016) have shown that silver ions in presence of citrated cyclodextrins after thermal treatment were converted into silver nanoparticles. In the same way, Carapeto et al. (Carapeto et al., 2017) proved the slow formation (48 hours) of silver nanoparticles in the presence of chitosan which is in agreement with our observation. In addition, the functionalised textiles loaded with silver were desorbed in 6.5 M nitric acid solution after their impregnation in the silver solution, before and after the thermal treatment (Figure 3c). Silver nanoparticles present in the supernatants were revealed by the peaks appearing at 400 nm increase after thermal treatment. The absorption peak of silver in the range of 400 nm indicated that nanoparticles formation was induced by the thermal treatment. The peak intensities reveal that more silver was adsorbed by CD-CTR functionalized textiles compared to CHT-CTR functionalized textiles. This difference is attributed to higher amount of -COOH functions present in the textile in CD-functionalized samples ( $46 \mu\text{mol}/\text{cm}^2$ ) than in CHT functionalized samples ( $14 \mu\text{mol}/\text{cm}^2$ ).

All curves in figure 2a and 2b show a significant decrease of the weight gain upon the application of the third layer (layer #3) of the system, which correspond to the self-assembled CHT layer in the first step of the L-b-L process. Comparing with the silver-free support system (Figure 2a), this weight loss corresponds to the migration of silver into the CHT solution. This phenomenon could not be avoided whatever the impregnation time in the CHT solution (Figure 2b). However, in case of application of the thermal treatment after silver impregnation step, this weight gain decrease was no longer observed as displayed in figure 2c. Indeed, as mentioned above, the application of the heat treatment allowed the formation of stable nanoparticles on the textiles that reduced the silver release in the polyelectrolyte solutions used the dip coating process.

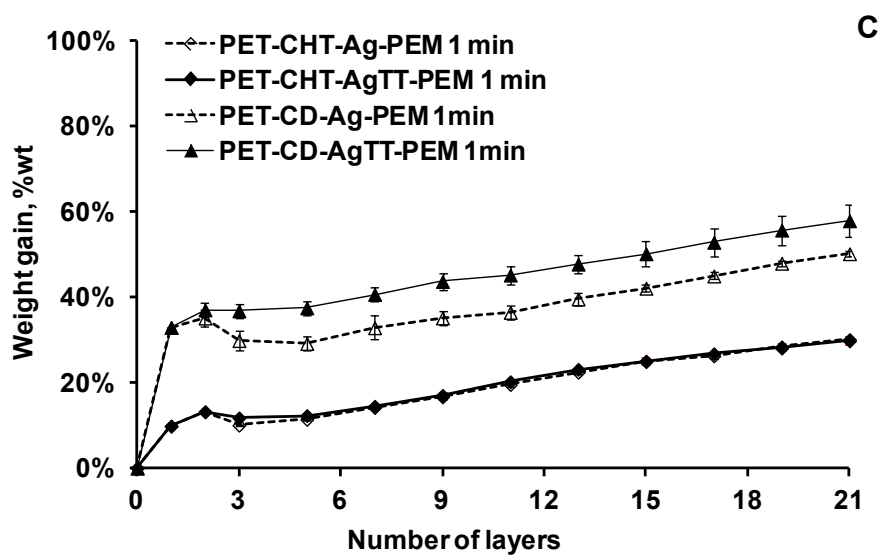
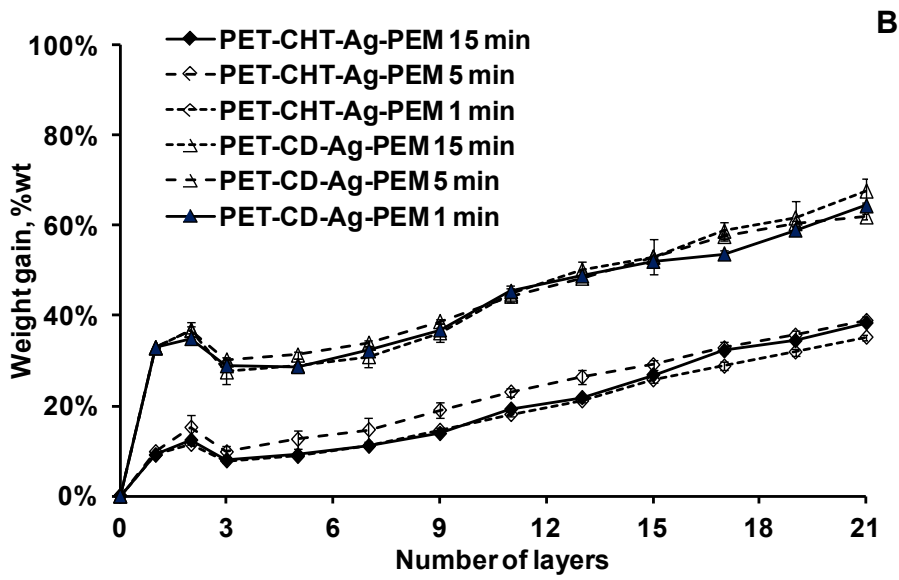
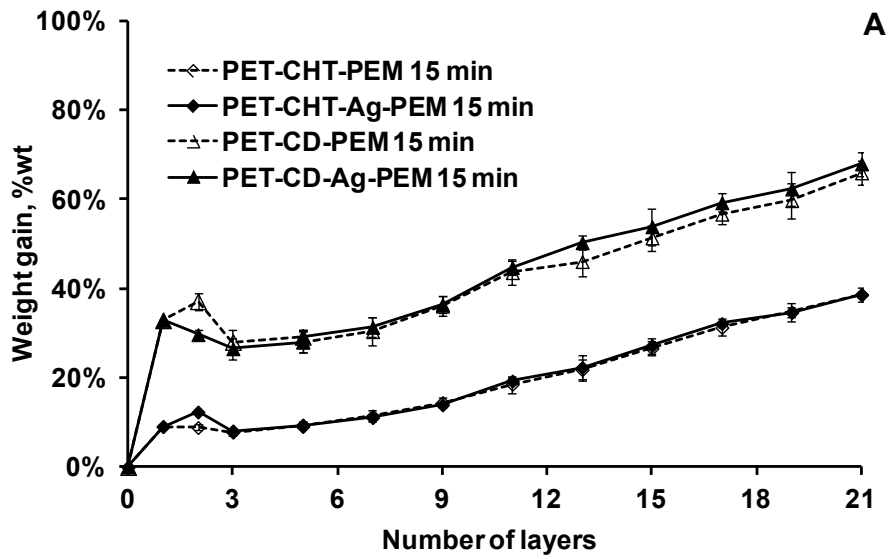
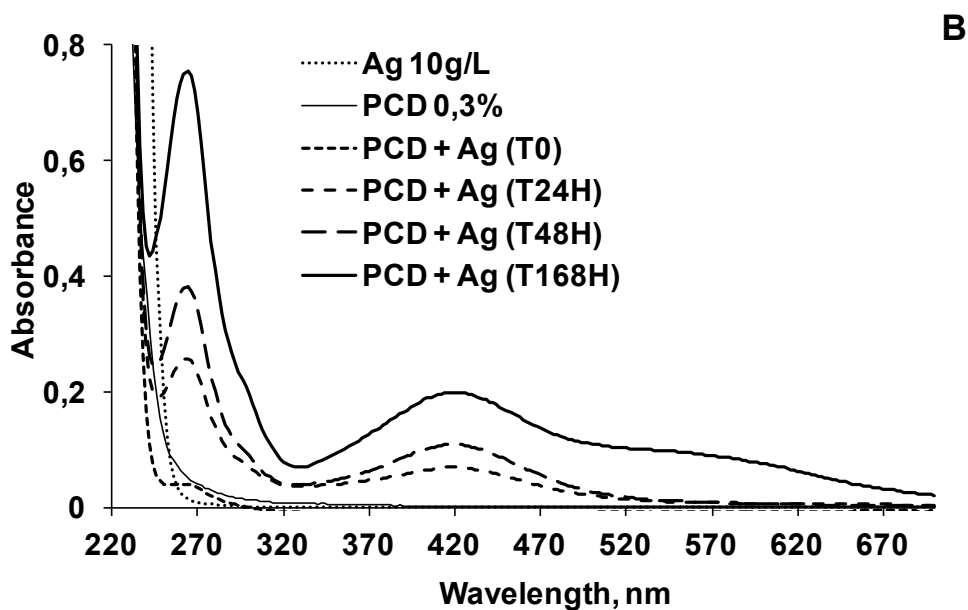
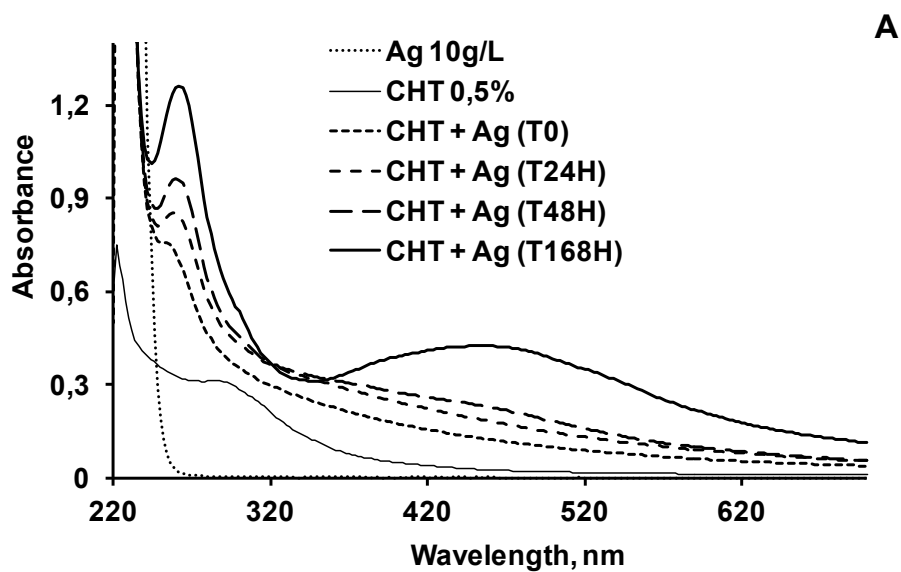


*Figure 2: Weight gain of textiles after pad/dry/cure step with citric acid and CHT or CD (layer #1), silver sulfate loading with or without Thermal Treatment (layer #2), and n cycles of layers depositions by L-b-L process in CHT solution (0.5% w/v) and in polyCTR-βCD solution (0.3% w/v) with dipping times of 1, 5 and 15 minutes.*

The L-b-L process was extended for PEM build-up by dip coating samples alternately in CHT and poly-cyclodextrin (PCD) solutions with intermediate rinsing and drying steps (Martin et al., 2013b, 2013a.). Figure 2 displays the linear evolution of the weight gain with the number of self-assembled bilayers on both functionalised and loaded textiles (Figure 2a). In particular, figure 2a displays that the presence of silver nanoparticles formed on the primer layers did not affect the PEM build-up. Moreover, figure 2b shows no influence of the time of impregnation (1, 5, 15 minutes) of samples in the dip-coating process. Indeed, the weight gain after the application of 21 layers reached respectively  $50 \pm 0.7\%$  and  $57 \pm 3.7\%$  for CD functionalized textiles loaded with silver with and without annealing. The same pattern is observed for L-b-L build-up on the CHT functionalized textile ( $30\% \pm 0.74\%$  vs  $29\% \pm 0.75\%$ ). The range of order of weight gain corresponding to the self-assembled CHT-PCD bilayers is the same for PEM coatings built on substrates modified with CHT and CD primer layers, so interestingly it is noteworthy that there is no influence of the support functionalization method on the subsequent PEM build-up.

As observed in figure 2, the weight gain of the textiles increased linearly with the number of deposited layers. Linear or exponential growth of LbL films has been widely discussed in literature. Linear regime is characterised by the adsorption of one polyelectrolyte by its self-deposition limited to the last oppositely charged deposited layer, while absorption by diffusion of the polyelectrolyte into the bulk of the LbL film provoking a charge overcompensation phenomenon occurs in the exponential regime. For a given polyelectrolytes couple, PEM build-up regime (linear or exponential) may depend on polymers parameters (weak/strong polyelectrolytes, molecular weight) solution parameters (concentration, pH, ionic strength) or process parameters (temperature or dipping time) (Dubas and Schlenoff, 2001; Seantier and Deratani, 2012; Volodkin and von Klitzing, 2014). LbL systems are ususally made from polyelectrolytes with linear chains, therefore it is difficult to compare our results with literature because if CHT is a linear chain, PCD presents a hyperbranched structure and forms globular nano-objects in the range of 50 nm diameter (Herbois et al., 2015) As a consequence, it is

unlikely that, due to its structure, PCD would diffuse inside the bulk of the PEM film, therefore this could explain the linear growth regime observed.





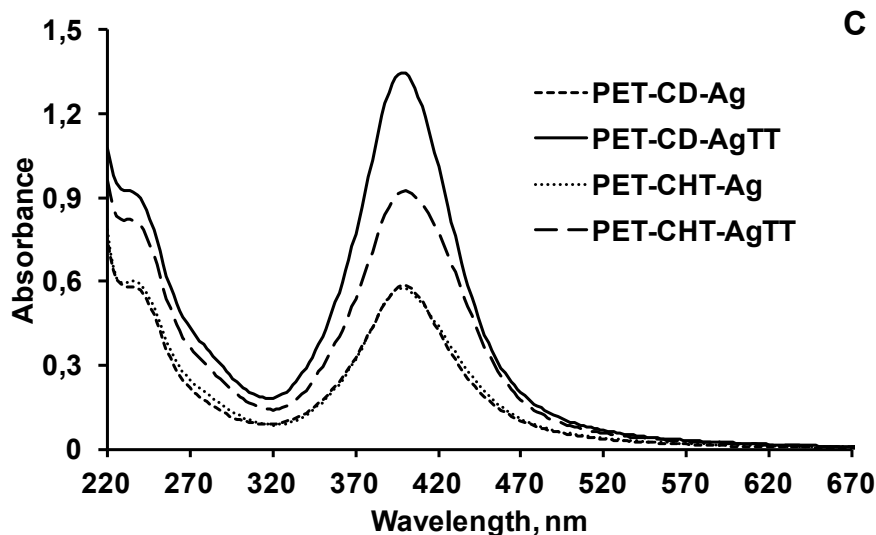
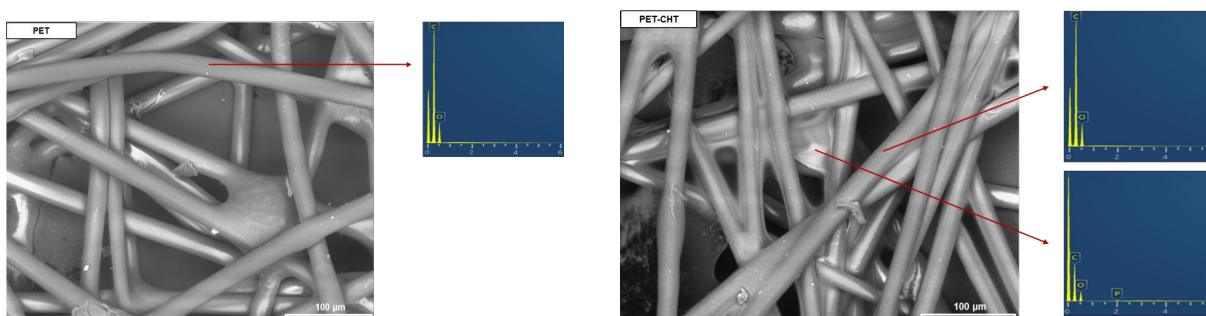


Figure 3. (a, b) UV-vis absorption spectra for the silver sulfate aqueous solution at 10 g/L, for the aqueous CHT solution at 0.5%, for the aqueous PCD solution at 0.3%, for the freshly prepared mixture of CHT 0.5% or PCD 0.3% with silver sulfate at 10 g/L, for 24h and 48 h later at room temperature. (b) UV-vis absorption spectra for textiles supports functionalized with CHT or PCD both loaded with silver before and after thermal treatment.

### 3.2. SEM/EDX evaluation

Figure 4 shows the morphology of CHT and CD functionalised textiles after pad/dry cure process loaded with silver and thermally treated. The presence of the primer pad/dry/cured layers polymer (CHT or CD) and the PEM coating can be easily observed on the micrographs. EDX spectra clearly confirm the presence of silver in the polymer coatings on the PET fibers after impregnation in silver solution and heating. However, the silver signal logically decreased in intensity after PEM deposition.



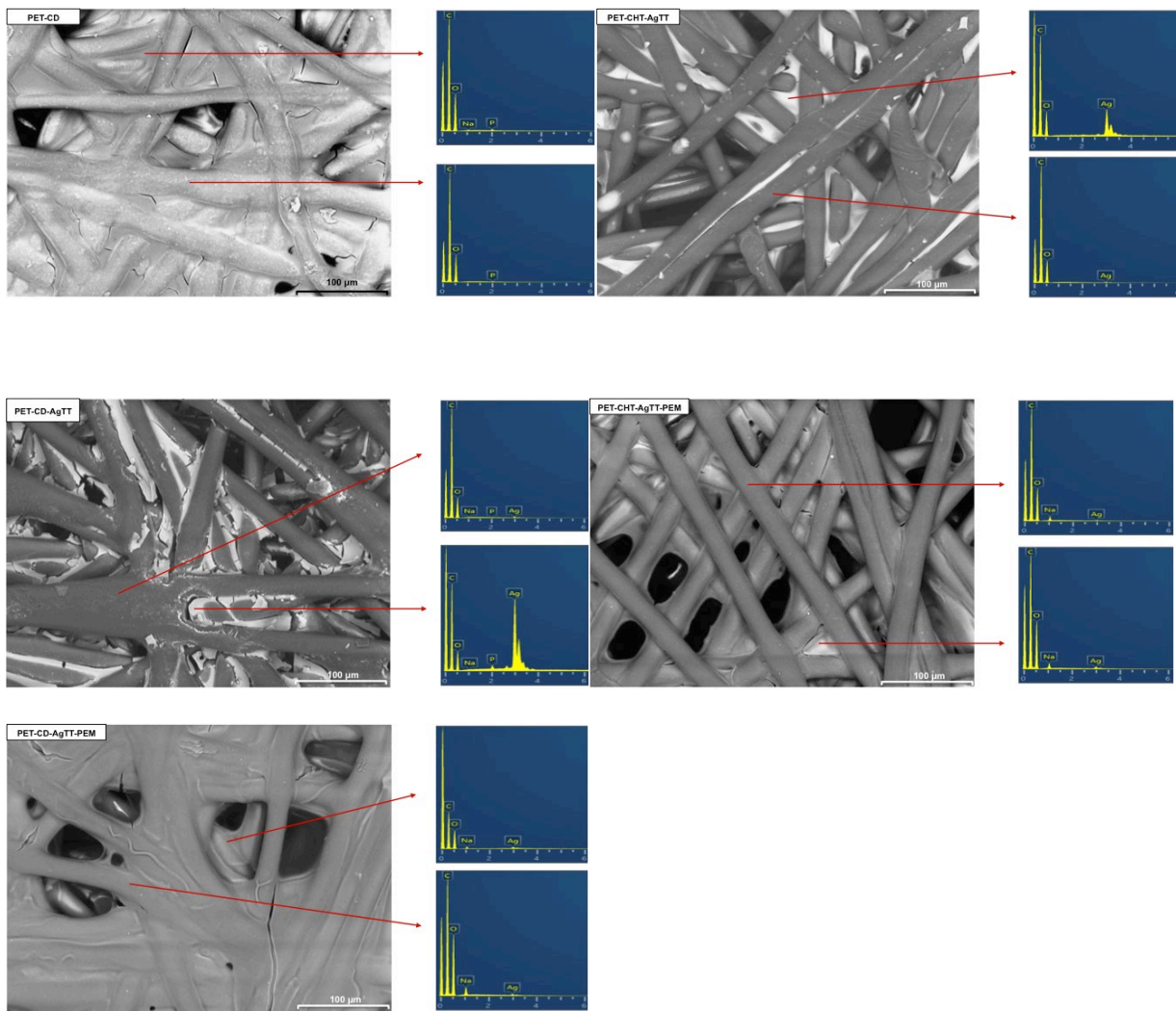


Figure 4. Representative SEM micrographs of textile samples tested with energy-dispersive X-ray spectroscopy (EDX) detector at the different stages of the elaboration. a) virgin textile, b) modified with CHT-CTR, c) modified with CD-CTR, e,f) after impregnation in silver sulfate and heating, g,h) after PEM deposition (21 layers),

### 3.3. Silver loading and silver release

Figure 5 shows the total amount of silver (measured by atomic absorption) on textiles at each stage of the process. A larger amount of silver was adsorbed by PCD functionalized textiles ( $450 \pm 28 \mu\text{g} / \text{cm}^2$ ) compared to those functionalized with CHT ( $289 \pm 40 \mu\text{g} / \text{cm}^2$ ). The values reached 429 and  $254 \mu\text{g}/\text{cm}^2$  respectively on the samples after the thermal treatment. This difference between CHT and CD treated samples for the primer layer deposition is directly related to their different carboxylic group densities as mentioned above. When the dip coating time was 15 minutes, the amount of silver on the functionalized textiles decreased sharply ( $30 \mu\text{g} / \text{cm}^2$  for PET-CD and  $4 \mu\text{g} / \text{cm}^2$  for PET-

CH), which is correlated to the decrease in mass gains observed in Figure 2. When the dip coating time was fixed to 1 min, the amount of silver on the textile decreased in a lesser extent compared to a time of 15 min ( $60 \mu\text{g} / \text{cm}^2$  for PET-CD,  $23 \mu\text{g} / \text{cm}^2$  for PET-CHT).

Interestingly, when applying the heat treatment after silver impregnation, the silver content reached 88 and  $210 \mu\text{g} / \text{cm}^2$  corresponding to a decrease of silver loss in the polyelectrolyte solutions during the dip-coating process. So, the combination of the thermal treatment applied to the silver layer with a short stay (1 minute) in the polyelectrolyte solutions during the L-b-L build-up process will be retained for the rest of the study in order to limit the silver loss.

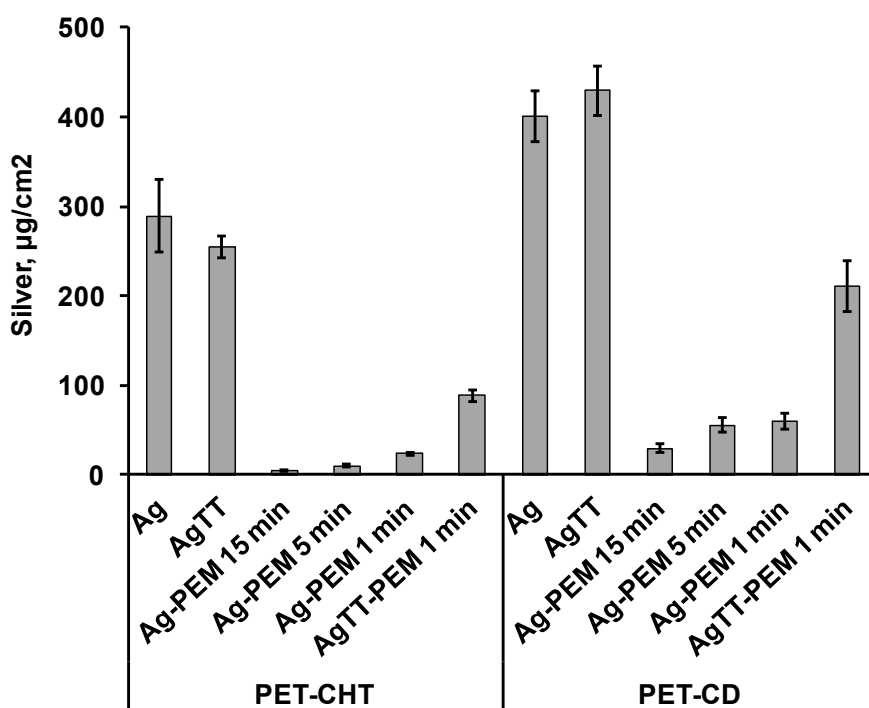


Figure 5: Silver amount on different textiles supports expressed in  $\mu\text{g}/\text{cm}^2$

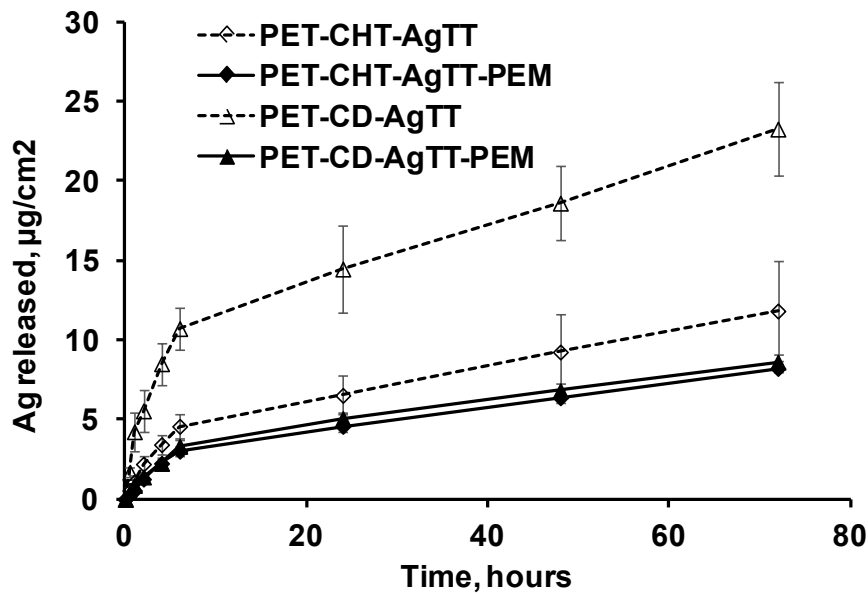


Figure 6: Release kinetics of silver expressed in  $\mu\text{g}/\text{cm}^2$  in PBS (pH7,4, 37°C, 80 rpm) from PET-CHT-AgTT, PET-CHT-AgTT-PEM, PET-CD-AgTT and PET-CD-AgTT-PEM textiles.

Figure 6 shows the release profiles of silver in PBS after soaking the samples pre-treated with CHT-CTR and CD-CTR, loaded with silver and heated, with or without the PEM system. CD-CTR textiles without PEM coating release the largest amount of silver ( $23.0 \pm 3 \mu\text{g} / \text{cm}^2$ ) after 3 days of immersion in PBS, corresponding to 5% of the initial silver loading. Interestingly, the multilayer system allows limiting the diffusion of silver in PBS to  $8.0 \pm 0.5 \mu\text{g} / \text{cm}^2$  in PBS, corresponding to 4% of the initial silver loading. The tendency is the same with CHT-CTR functionalised textiles loaded with silver (respectively  $12.0 \pm 3$  and  $8.0 \pm 0.26 \mu\text{g} / \text{cm}^2$  with or without the multilayer system). These result displays that the multilayer coating allows slowing down the diffusion of silver in PBS and acts as a barrier. This phenomenon was observed elsewhere by (Soltani et al., 2017) with a multilayer system containing polyethyleneimine (PEI) and poly (ethylene terephthalate) ionomer (PETi). In this case, a decrease in terms of the permeability to carbon dioxide and oxygen was observed.

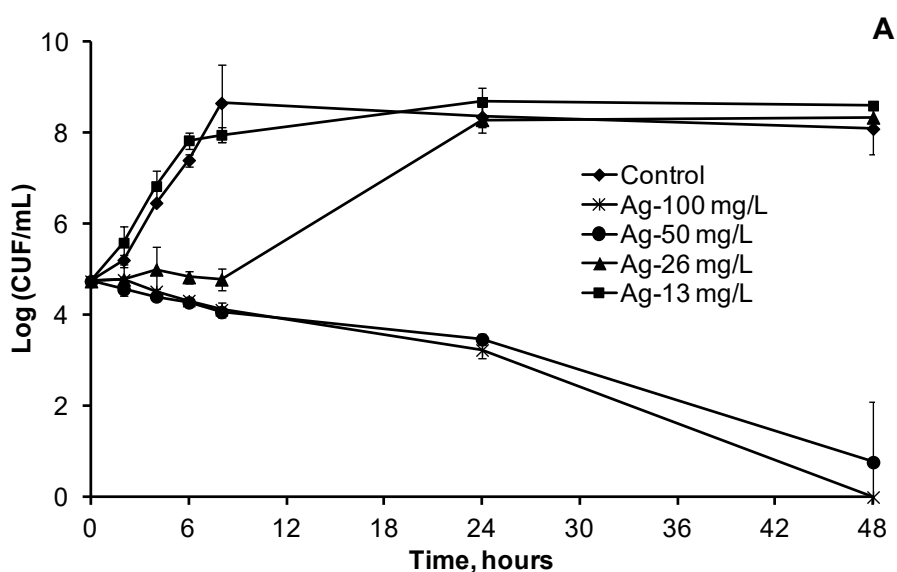
In our case, the silver release in PBS represents only 4 to 5% of the total amount of silver containing in the textiles without the multilayer system and 4 to 10 % in textiles with the multilayer system. This control of silver release is important as silver diffusion in living tissues is considered as a cause of cytotoxicity. As a matter of fact, many studies evaluate the cytotoxicity of silver ions and silver

nanoparticles, Barbasz et al. clearly proved that the cytotoxicity of silver is cell type-dependent and particles size dependent (Barbasz et al., 2017). To summarize, a silver cytotoxicity was observed in the range 0.1 to 10 mg/L (Akter et al., 2018), but this cytotoxicity decrease when silver was associated with a polymer chemically interacting with silver and reduces thereby its diffusion (100 mg/L) (Lu et al., 2010). It is really important to be below this threshold of toxicity by maintaining an antibacterial activity of the dressing.

### 3.4. Microbiological evaluation

Minimal Inhibitory Concentration (MIC) was determined against *S. aureus* and *E. coli* exposed to decreasing silver sulphate concentrations (from 400 mg/L to 0.06 µg/L). Results show that silver is more effective against *E. coli* than *S. aureus*, presenting respectively a MIC of 25 mg/L versus 50 mg/L measured at 48 hours (Kędziora et al., 2018; Krishnaraj et al., 2010).

The growth curves of both bacterial strains in presence of silver concentrations approaching the MIC concentration were established. Figure 7a indicates that silver concentrations above or equal to 26 mg/L could inhibit the growth of *S. aureus* for up to 8 hours. However, the biocidal effect was confirmed only for silver concentrations above 50mg/L at 24 and 48 hours. Silver concentrations equal to 50 mg/L presented biocidal activity against *E. coli* during up to 8 hours, then bacteria proliferated again (Figure 7b).



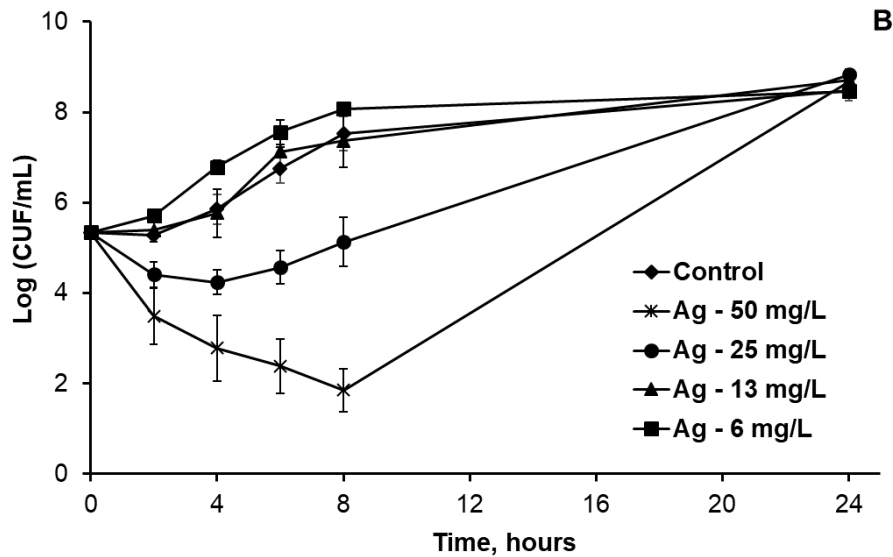


Figure 7: Growth curve of *S. aureus* (a) and *E. coli* (b) in presence of different concentrations of silver sulfate

The antibacterial activity of textiles was assessed by the Kirby-Bauer tests. Figures 8a and 8b report the inhibition zones diameters around freshly prepared samples and samples after immersion in PBS media for 72 hours, against *S. aureus* and *E. coli* respectively. No intrinsic antibacterial activity was observed for samples without preliminary activation with silver salt on contrary of samples loaded with silver, with or without PEM coating. CHT-CTR functionalized textile (PET-CHT-AgTT) showed an inhibition diameter of  $15 \pm 0.5$  mm on *S. aureus* at 0 and 72 hours respectively and an inhibition diameter of  $15.5 \pm 0.5$  mm on *E. coli* at 72 hours. In the same way, CD-CTR functionalized textiles (PET-CD-AgTT) showed an inhibition diameter of  $17 \pm 2.8$  mm at the beginning of the test which decrease slightly to  $15 \pm 1.03$  mm after 72 hours for *S. aureus* and  $16 \pm 1.03$  mm for *E. coli* respectively. In the other hand, when the PEM system was applied the inhibition zone decreased due to slow release rate of silver from textile samples showing a diameter of  $14 \pm 1.21$  mm against *S. aureus* and  $13.8 \pm 0.75$  mm against *E. coli* for PET-CHT-AgTT-PEM textiles at 0 and 72 hours. For the last group, PET-CD-AgTT-PEM, the inhibition diameter was of  $14.5 \pm 0.8$  mm and  $15.5 \pm 1.0$  mm against *S. aureus* and *E. coli* at 0 and 72 hours respectively. The dressing developed in this work show inhibition diameters against *S. aureus* and *E. coli* similar to other different wound dressing materials which also presents silver nanoparticles padded in viscose (Montaser et al., 2016) and cotton (Hebeish et al., 2014) or incorporated by plasma treatment in flax (Paladini et al., 2015).

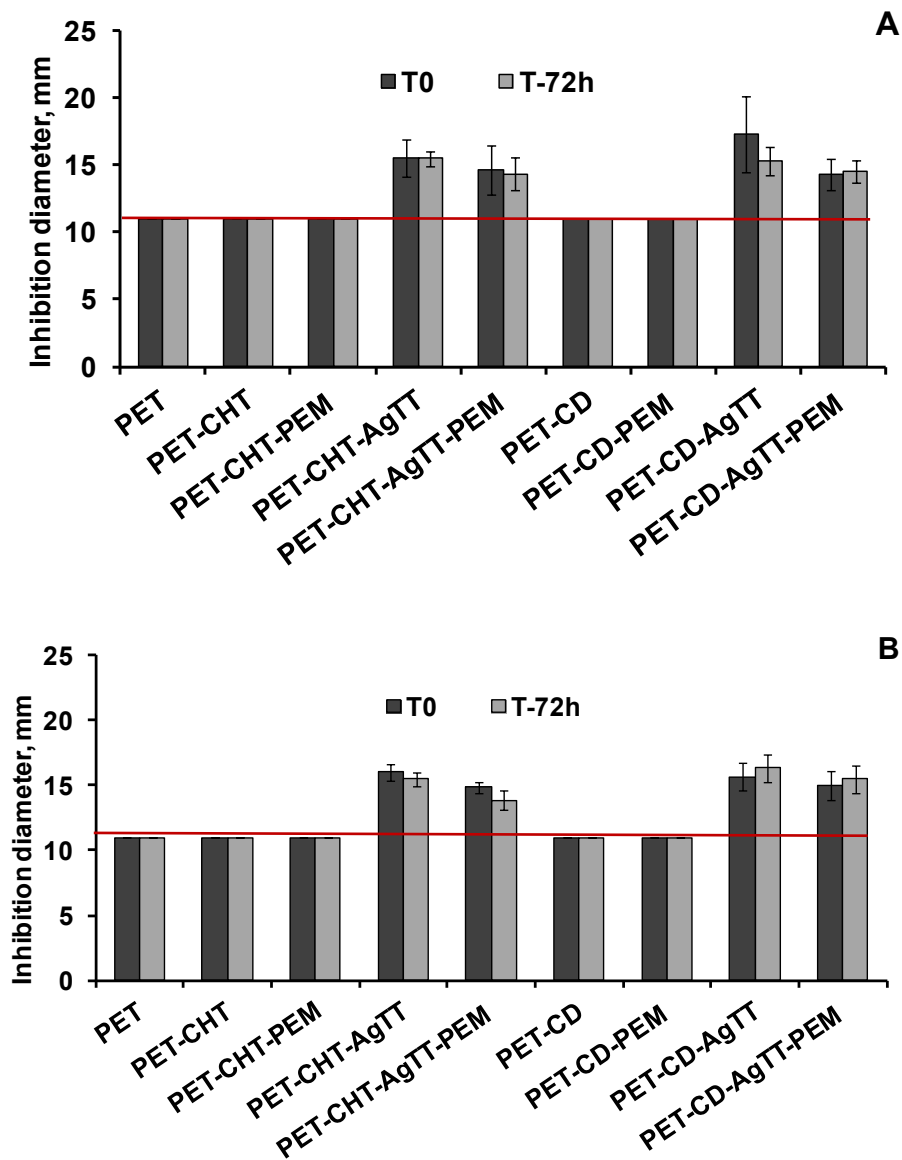
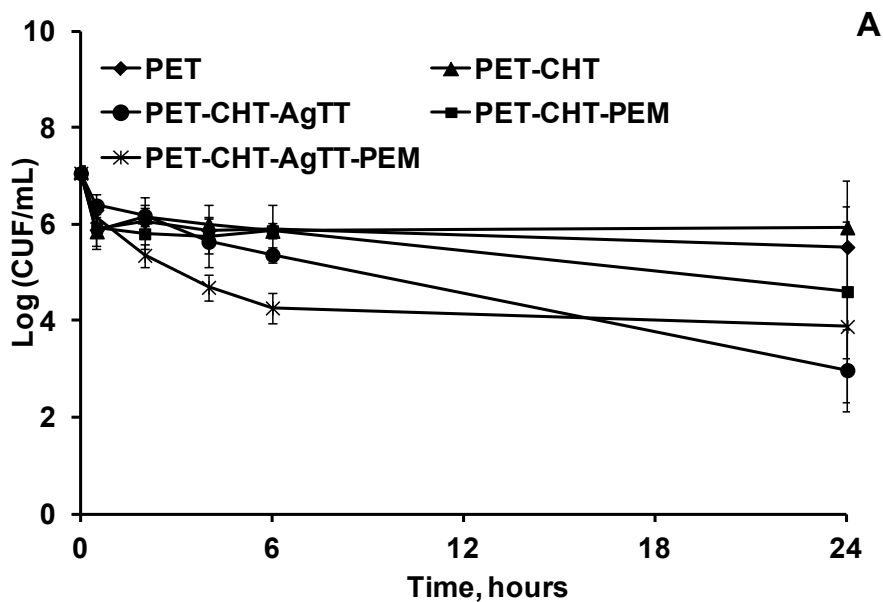


Figure 8: Inhibition diameter in the Kirby–Bauer test against *S. aureus* (a) or *E. coli* (b) of textile samples at 0 after 72 hours in PBS pH 7.4 media. The red line in the graph indicates the diameter of the textile samples (11 mm) placed onto Muller-Hinton agar.

Bacterial reduction test (*Kill Time Test*) was performed in order to evaluate the antibacterial activity of different textiles supports and to measure the rate at which textiles samples inhibit the bacterial proliferation. Fig. 9 shows the bacterial reduction expressed on log CFU/mL of *S. aureus* (9a and b) and *E. coli* (9c and d) that were in contact with textiles samples for different times (from 0.5 to 24 hours). Samples without silver loading did not present any antibacterial activity against both strains. In contrast, CHT-CTR and CD-CTR pre-treated textiles loaded with silver displayed a bacterial reduction of 4 log<sub>10</sub> and 6 log<sub>10</sub> against *S. aureus* and a bacterial reduction of 6 log<sub>10</sub> and 5 log<sub>10</sub>

against *E. coli* at 24 hours respectively. In the case of textiles coated by the PEM system, the antibacterial activity on both strains is more sustained presenting a bacterial reduction of 3 log<sub>10</sub> and 5 log<sub>10</sub> at 24 hours against *S. aureus* and *E. coli* respectively. It is noteworthy that CD-CTR pre-treated textiles loaded with silver displayed a higher antibacterial activity than those pre-treated by CHT-CTR due to the higher silver sorption capacity of these supports as discussed above (Figure 5). In addition, the antibacterial activity of samples is faster against *E. coli* than against *S. aureus* irrespectively of the textile sample tested. Indeed, kill time tests profiles display a maximal bacterial reduction within the first 5 hours of contact with *E. coli* while a progressive reduction extended up to 24 hours was observed with *S. aureus*.





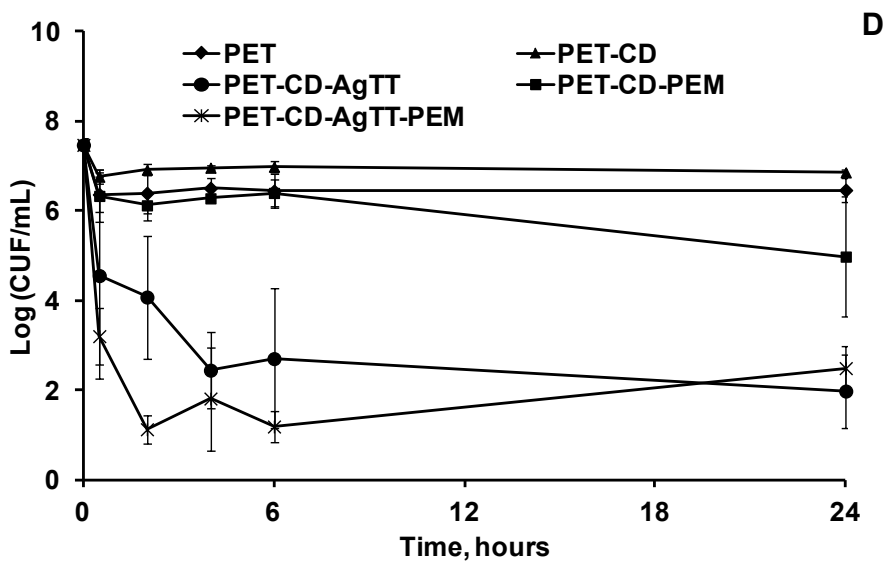
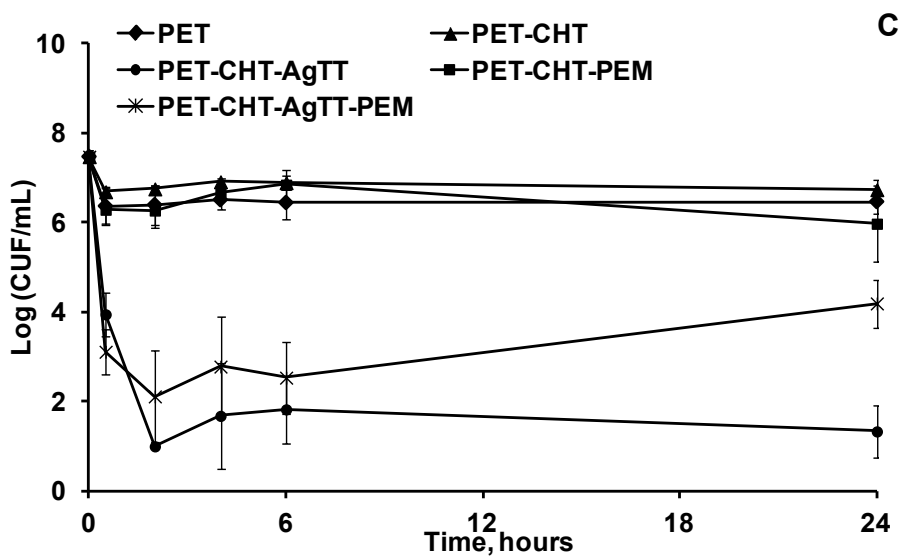
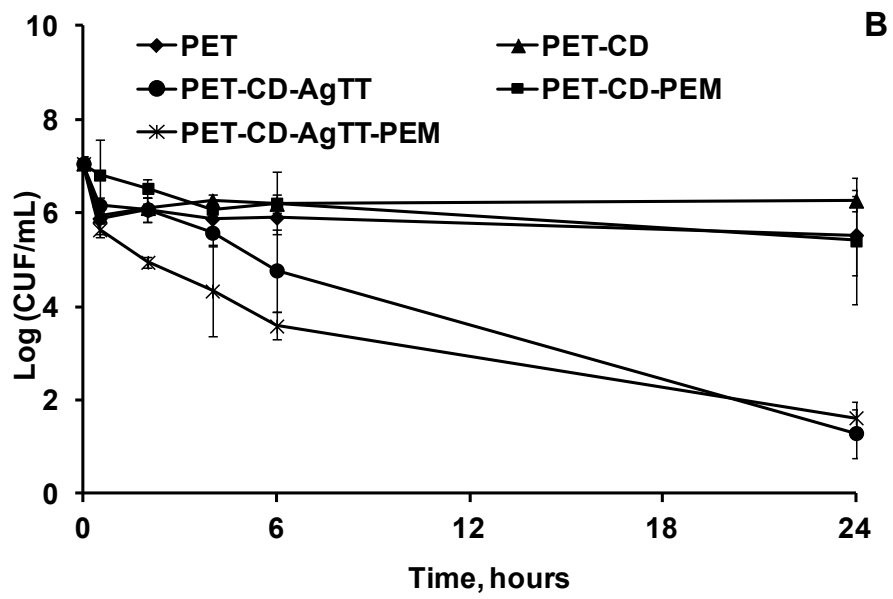


Figure 9: Kinetic bacterial reduction *S. aureus* (a, b) or *E. coli* (c, d) in contact with textiles supports

The development of PEM system based wound dressing as drug delivery systems is flourishing. In this case, the objective is to incorporate antimicrobials drugs (i.e. silver) to obtain a local controlled release into the infected wound. In many works, silver is incorporated into assemblies at the end of PEM build-up with allow silver diffusion (Sripriya et al., 2013; Anandhakumar and Raichur, 2013). They observed an antibacterial activity of PEM containing silver using a diffusion test. Indeed, this test reveal an important diffusion of silver from PEM. The aim of our work was to entrap silver on the first layer and then develop the PEM system in order to form a barrier that avoid silver diffusion and reduce silver toxicity in the wound. Interestingly, they also observed that the antibacterial activity of these PEM containg silver can be improve with the association of antibiotics as a moxifloxacin or ciprofloxacin against *S. aureus* and *E. coli* respectively. This strategy could be apply on our wound dressing to improve efficacy of treatment of infected chronic wound.

## **Conclusion**

polyethylene terephthalate (PET) nonwovens were pre-treated by two types of polysaccharides – CHT and CD – crosslinked with citric acid by a pad/dry/cure process. Both types of thermofixed supports presented an anionic character thanks to the presence of residual carboxylate groups carried by the citrate crosslinks. Samples were then loaded by soaking in silver sulfate solution. The silver cations sorption occurred by ion exchange capacity of samples and was more extended for CD-CTR pretreated samples compared to CHT-CTR ones. We have observed that the thermal treatment step after silver loading provoked the formation of silver nanoparticles that prevented silver leakage from samples in the CHT and PCD solutions during the L-b-L process. The self-assembly of chitosan and PCD bilayers on the textile surface was not affected by the presence of silver entrapped in primer anionic layer. Liberation tests showed that the PEM coating slowed down the silver release in batch but did not affect the antibacterial activity as observed by Kirby-Bauer and *kill time* tests. Samples presented antibacterial activity against both *S. aureus* and *E coli* with a faster efficacy on the later strain. This dressing concept has a real potential for the prevention of wound infections by limiting the diffusion of silver in the wound and its side effects. This should be considered in the future through animal tests. Besides, some works are in progress concerning the loading of a second drug

(anti-inflammatory or antibacterial agents) in the empty CD cavities present in the PEM system in order to provide a dual therapeutic action).

## References:

- Abboud, E.C., Settle, J.C., Legare, T.B., Marcet, J.E., Barillo, D.J., Sanchez, J.E., 2014. Silver-based dressings for the reduction of surgical site infection: Review of current experience and recommendation for future studies. *Burns* 40, S30–S39. <https://doi.org/10.1016/j.burns.2014.09.011>
- Abdel-Mohsen, A.M., Jancar, J., Abdel-Rahman, R.M., Vojtek, L., Hyršl, P., Dušková, M., Nejezchlebová, H., 2017. A novel in situ silver/hyaluronan bio-nanocomposite fabrics for wound and chronic ulcer dressing: In vitro and in vivo evaluations. *Int. J. Pharm.* 520, 241–253. <https://doi.org/10.1016/j.ijpharm.2017.02.003>
- Abdel-Rahman, R.M., Abdel-Mohsen, A.M., Hrdina, R., Burgert, L., Fohlerova, Z., Pavlišák, D., Sayed, O.N., Jancar, J., 2016. Wound dressing based on chitosan/hyaluronan/nonwoven fabrics: Preparation, characterization and medical applications. *Int. J. Biol. Macromol.* 89, 725–736. <https://doi.org/10.1016/j.ijbiomac.2016.04.087>
- Agarwal, A., Nelson, T.B., Kierski, P.R., Schurr, M.J., Murphy, C.J., Czuprynski, C.J., McAnulty, J.F., Abbott, N.L., 2012. Polymeric multilayers that localize the release of chlorhexidine from biologic wound dressings. *Biomaterials* 33, 6783–6792. <https://doi.org/10.1016/j.biomaterials.2012.05.068>
- Akter, M., Sikder, M.T., Rahman, M.M., Ullah, A.K.M.A., Hossain, K.F.B., Banik, S., Hosokawa, T., Saito, T., Kurasaki, M., 2018. A systematic review on silver nanoparticles-induced cytotoxicity: Physicochemical properties and perspectives. *J. Adv. Res.* 9, 1–16. <https://doi.org/10.1016/j.jare.2017.10.008>
- Anandhakumar, S., Raichur, A.M., 2013. Polyelectrolyte/silver nanocomposite multilayer films as multifunctional thin film platforms for remote activated protein and drug delivery. *Acta Biomater.* 9, 8864–8874. <https://doi.org/10.1016/j.actbio.2013.06.012>
- Atiyeh, B.S., Costagliola, M., Hayek, S.N., Dibo, S.A., 2007. Effect of silver on burn wound infection control and healing: Review of the literature. *Burns* 33, 139–148. <https://doi.org/10.1016/j.burns.2006.06.010>
- Aubert-Viard, F., Martin, A., Chai, F., Neut, C., Tabary, N., Martel, B., Nicolas Blanchemain, 2015. Chitosan finishing nonwoven textiles loaded with silver and iodide for antibacterial wound dressing applications. *Biomed. Mater.* 10, 015023.
- Barbasz, A., Oćwieja, M., Roman, M., 2017. Toxicity of silver nanoparticles towards tumoral human cell lines U-937 and HL-60. *Colloids Surf. B Biointerfaces* 156, 397–404. <https://doi.org/10.1016/j.colsurfb.2017.05.027>
- Bhowmick, S., Koul, V., 2016. Assessment of PVA/silver nanocomposite hydrogel patch as antimicrobial dressing scaffold: Synthesis, characterization and biological evaluation. *Mater. Sci. Eng. C* 59, 109–119. <https://doi.org/10.1016/j.msec.2015.10.003>
- Brewster, M.E., Loftsson, T., 2007. Cyclodextrins as pharmaceutical solubilizers. *Adv. Drug Deliv. Rev.* 59, 645–666. <https://doi.org/10.1016/j.addr.2007.05.012>
- Burd, A., Kwok, C.H., Hung, S.C., Chan, H.S., Gu, H., Lam, W.K., Huang, L., 2007. A comparative study of the cytotoxicity of silver-based dressings in monolayer cell, tissue explant, and animal models. *Wound Repair Regen.* 15, 94–104. <https://doi.org/10.1111/j.1524-475X.2006.00190.x>

- Carapeto, A.P., Ferraria, A.M., do Rego, A.M.B., 2017. Unraveling the reaction mechanism of silver ions reduction by chitosan from so far neglected spectroscopic features. *Carbohydr. Polym.* 174, 601–609. <https://doi.org/10.1016/j.carbpol.2017.06.100>
- Croisier, F., Jérôme, C., 2013. Chitosan-based biomaterials for tissue engineering. *Eur. Polym. J.* 49, 780–792. <https://doi.org/10.1016/j.eurpolymj.2012.12.009>
- Danel, C., Azaroual, N., Chavaria, C., Odou, P., Martel, B., Vaccher, C., 2013. Comparative study of the complex forming ability and enantioselectivity of cyclodextrin polymers by CE and <sup>1</sup>H NMR. *Carbohydr. Polym.* 92, 2282–2292. <https://doi.org/10.1016/j.carbpol.2012.11.095>
- Decher, G., 1997. Fuzzy Nanoassemblies: Toward Layered Polymeric Multicomposites. *Science* 277, 1232–1237. <https://doi.org/10.1126/science.277.5330.1232>
- Decher, G., Ecker, M., Schmitt, J., Struth, B., 1998. Layer-by-layer assembled multicomposite films. *Curr. Opin. Colloid Interface Sci.* 3, 32–39. [https://doi.org/10.1016/S1359-0294\(98\)80039-3](https://doi.org/10.1016/S1359-0294(98)80039-3)
- Dubas, S.T., Schlenoff, J.B., 2001. Polyelectrolyte Multilayers Containing a Weak Polyacid: Construction and Deconstruction. *Macromolecules* 34, 3736–3740. <https://doi.org/10.1021/ma001720t>
- Fahmy, H.M., Aly, A.A., Abou-Okeil, A., 2018. A non-woven fabric wound dressing containing layer – by – layer deposited hyaluronic acid and chitosan. *Int. J. Biol. Macromol.* 114, 929–934. <https://doi.org/10.1016/j.ijbiomac.2018.03.149>
- García-Fernández, M.J., Tabary, N., Martel, B., Cazaux, F., Oliva, A., Taboada, P., Concheiro, A., Alvarez-Lorenzo, C., 2013. Poly-(cyclo)dextrins as ethoxzolamide carriers in ophthalmic solutions and in contact lenses. *Carbohydr. Polym.* 98, 1343–1352. <https://doi.org/10.1016/j.carbpol.2013.08.003>
- Gomes, A.P., Mano, J.F., Queiroz, J.A., Gouveia, I.C., 2015. Incorporation of antimicrobial peptides on functionalized cotton gauzes for medical applications. *Carbohydr. Polym.* 127, 451–461. <https://doi.org/10.1016/j.carbpol.2015.03.089>
- Halstead, F.D., Rauf, M., Bamford, A., Wearn, C.M., Bishop, J.R.B., Burt, R., Fraise, A.P., Moiemmen, N.S., Oppenheim, B.A., Webber, M.A., 2015. Antimicrobial dressings: Comparison of the ability of a panel of dressings to prevent biofilm formation by key burn wound pathogens. *Burns* 41, 1683–1694. <https://doi.org/10.1016/j.burns.2015.06.005>
- Han, F., Dong, Y., Song, A., Yin, R., Li, S., 2014. Alginate/chitosan based bi-layer composite membrane as potential sustained-release wound dressing containing ciprofloxacin hydrochloride. *Appl. Surf. Sci.* 311, 626–634. <https://doi.org/10.1016/j.apsusc.2014.05.125>
- Hebeish, A., El-Rafie, M.H., EL-Sheikh, M.A., Seleem, A.A., El-Naggar, M.E., 2014. Antimicrobial wound dressing and anti-inflammatory efficacy of silver nanoparticles. *Int. J. Biol. Macromol.* 65, 509–515. <https://doi.org/10.1016/j.ijbiomac.2014.01.071>
- Herbois, R., Noël, S., Léger, B., Tilloy, S., Menuel, S., Addad, A., Martel, B., Ponchel, A., Monflier, E., 2015. Ruthenium-containing  $\beta$ -cyclodextrin polymer globules for the catalytic hydrogenation of biomass-derived furanic compounds. *Green Chem.* 17, 2444–2454. <https://doi.org/10.1039/C5GC00005J>
- Ito, K., Saito, A., Fujie, T., Nishiwaki, K., Miyazaki, H., Kinoshita, M., Saitoh, D., Ohtsubo, S., Takeoka, S., 2015. Sustainable antimicrobial effect of silver sulfadiazine-loaded nanosheets on infection in a mouse model of partial-thickness burn injury. *Acta Biomater.* 24, 87–95. <https://doi.org/10.1016/j.actbio.2015.05.035>

- Jhass, P., Siaw-Sakyi, V., Wild, T., 2017. Wound infection risk evaluation – a new prediction score – WIRE. *Wound Med.* 16, 34–39. <https://doi.org/10.1016/j.wndm.2017.02.001>
- Kędziora, A., Speruda, M., Krzyżewska, E., Rybka, J., Łukowiak, A., Bugla-Płoskońska, G., 2018. Similarities and Differences between Silver Ions and Silver in Nanoforms as Antibacterial Agents. *Int. J. Mol. Sci.* 19, 444. <https://doi.org/10.3390/ijms19020444>
- Krishnaraj, C., Jagan, E.G., Rajasekar, S., Selvakumar, P., Kalaichelvan, P.T., Mohan, N., 2010. Synthesis of silver nanoparticles using *Acalypha indica* leaf extracts and its antibacterial activity against water borne pathogens. *Colloids Surf. B Biointerfaces* 76, 50–56. <https://doi.org/10.1016/j.colsurfb.2009.10.008>
- Leaper, D., MacGregor, L., 2012. Appropriate use of silver dressings in wounds: International consensus document. *Int. Wound J.* 9, 461–464. <https://doi.org/10.1111/j.1742-481X.2012.01091.x>
- Lee, Y.-H., Chang, J.-J., Yang, M.-C., Chien, C.-T., Lai, W.-F., 2012. Acceleration of wound healing in diabetic rats by layered hydrogel dressing. *Carbohydr. Polym.* 88, 809–819. <https://doi.org/10.1016/j.carbpol.2011.12.045>
- Lu, W., Senapati, D., Wang, S., Tovmachenko, O., Singh, A.K., Yu, H., Ray, P.C., 2010. Effect of surface coating on the toxicity of silver nanomaterials on human skin keratinocytes. *Chem. Phys. Lett.* 487, 92–96. <https://doi.org/10.1016/j.cplett.2010.01.027>
- Ma, Q., Song, J., Zhang, S., Wang, M., Guo, Y., Dong, C., 2016. Colorimetric detection of riboflavin by silver nanoparticles capped with  $\beta$ -cyclodextrin-grafted citrate. *Colloids Surf. B Biointerfaces* 148, 66–72. <https://doi.org/10.1016/j.colsurfb.2016.08.040>
- Martel, B., Morcellet, M., Ruffin, D., Ducoroy, L., Weltrowski, M., 2002. Finishing of Polyester Fabrics with Cyclodextrins and Polycarboxylic Acids as Crosslinking Agents. *J. Incl. Phenom. Macrocycl. Chem.* 44, 443–446. <https://doi.org/10.1023/A:1023080221850>
- Martin, A., Tabary, N., Chai, F., Leclercq, L., Junthip, J., Aubert-Viard, F., Neut, C., Weltrowski, M., Blanchemain, N., Martel, B., 2013a. Build-up of an antimicrobial multilayer coating on a textile support based on a methylene blue–poly(cyclodextrin) complex. *Biomed. Mater.* 8, 065006. <https://doi.org/10.1088/1748-6041/8/6/065006>
- Martin, A., Tabary, N., Leclercq, L., Junthip, J., Degoutin, S., Aubert-Viard, F., Cazaux, F., Lyskawa, J., Janus, L., Bria, M., Martel, B., 2013b. Multilayered textile coating based on a  $\beta$ -cyclodextrin polyelectrolyte for the controlled release of drugs. *Carbohydr. Polym.* 93, 718–730. <https://doi.org/10.1016/j.carbpol.2012.12.055>
- Marx, D.E., Barillo, D.J., 2014. Silver in medicine: The basic science. *Burns* 40, S9–S18. <https://doi.org/10.1016/j.burns.2014.09.010>
- Maver, T., Gradišnik, L., Kurečič, M., Hribernik, S., Smrke, D.M., Maver, U., Kleinschek, K.S., 2017. Layering of different materials to achieve optimal conditions for treatment of painful wounds. *Int. J. Pharm.* 529, 576–588. <https://doi.org/10.1016/j.ijpharm.2017.07.043>
- Maver, T., Hribernik, S., Mohan, T., Smrke, D.M., Maver, U., Stana-Kleinschek, K., 2015. Functional wound dressing materials with highly tunable drug release properties. *RSC Adv.* 5, 77873–77884. <https://doi.org/10.1039/C5RA11972C>
- Montaser, A.S., Abdel-Mohsen, A.M., Ramadan, M.A., Sleem, A.A., Sahffie, N.M., Jancar, J., Hebeish, A., 2016. Preparation and characterization of alginate/silver/nicotinamide nanocomposites for treating diabetic wounds. *Int. J. Biol. Macromol.* 92, 739–747. <https://doi.org/10.1016/j.ijbiomac.2016.07.050>

- Paladini, F., Picca, R.A., Sportelli, M.C., Cioffi, N., Sannino, A., Pollini, M., 2015. Surface chemical and biological characterization of flax fabrics modified with silver nanoparticles for biomedical applications. *Mater. Sci. Eng. C* 52, 1–10. <https://doi.org/10.1016/j.msec.2015.03.035>
- Poon, V.K.M., Burd, A., 2004. In vitro cytotoxicity of silver: implication for clinical wound care. *Burns* 30, 140–147. <https://doi.org/10.1016/j.burns.2003.09.030>
- Rai, M.K., Deshmukh, S.D., Ingle, A.P., Gade, A.K., 2012. Silver nanoparticles: the powerful nanoweapon against multidrug-resistant bacteria: Activity of silver nanoparticles against MDR bacteria. *J. Appl. Microbiol.* 112, 841–852. <https://doi.org/10.1111/j.1365-2672.2012.05253.x>
- Seantier, B., Deratani, A., 2012. Polyelectrolytes at Interfaces: Applications and Transport Properties of Polyelectrolyte Multilayers in Membranes, in: *Ionic Interactions in Natural and Synthetic Macromolecules*. Wiley-Blackwell, pp. 683–726. <https://doi.org/10.1002/9781118165850.ch18>
- Shukla, A., Fang, J.C., Puranam, S., Hammond, P.T., 2012. Release of vancomycin from multilayer coated absorbent gelatin sponges. *J. Controlled Release* 157, 64–71. <https://doi.org/10.1016/j.jconrel.2011.09.062>
- Shukla, A., Fuller, R.C., Hammond, P.T., 2011. Design of multi-drug release coatings targeting infection and inflammation. *J. Controlled Release* 155, 159–166. <https://doi.org/10.1016/j.jconrel.2011.06.011>
- Soltani, I., Smith, S.D., Spontak, R.J., 2017. Effect of polyelectrolyte on the barrier efficacy of layer-by-layer nanoclay coatings. *J. Membr. Sci.* 526, 172–180. <https://doi.org/10.1016/j.memsci.2016.12.022>
- Sripriya, J., Anandhakumar, S., Achiraman, S., Antony, J.J., Siva, D., Raichur, A.M., 2013. Laser receptive polyelectrolyte thin films doped with biosynthesized silver nanoparticles for antibacterial coatings and drug delivery applications. *Int. J. Pharm.* 457, 206–213. <https://doi.org/10.1016/j.ijpharm.2013.09.036>
- Tabary, N., Garcia-Fernandez, M.J., Danède, F., Descamps, M., Martel, B., Willart, J.-F., 2016. Determination of the glass transition temperature of cyclodextrin polymers. *Carbohydr. Polym.* 148, 172–180. <https://doi.org/10.1016/j.carbpol.2016.04.032>
- Trinca, R.B., Westin, C.B., da Silva, J.A.F., Moraes, Â.M., 2017. Electrospun multilayer chitosan scaffolds as potential wound dressings for skin lesions. *Eur. Polym. J.* 88, 161–170. <https://doi.org/10.1016/j.eurpolymj.2017.01.021>
- Volodkin, D., von Klitzing, R., 2014. Competing mechanisms in polyelectrolyte multilayer formation and swelling: Polycation–polyanion pairing vs. polyelectrolyte–ion pairing. *Curr. Opin. Colloid Interface Sci.* 19, 25–31. <https://doi.org/10.1016/j.cocis.2014.01.001>
- Wijesena, R.N., Tissera, N.D., Abeyratne, C., Bangamuwa, O.M., Ludowyke, N., Dahanayake, D., Gunasekara, S., de Silva, N., de Silva, R.M., de Silva, K.M.N., 2017. In-situ formation of supramolecular aggregates between chitin nanofibers and silver nanoparticles. *Carbohydr. Polym.* 173, 295–304. <https://doi.org/10.1016/j.carbpol.2017.05.065>
- Zhang, J., Ma, P.X., 2013. Cyclodextrin-based supramolecular systems for drug delivery: Recent progress and future perspective. *Adv. Drug Deliv. Rev.* 65, 1215–1233. <https://doi.org/10.1016/j.addr.2013.05.001>